

A Biodegradable Composite Scaffold Prepared Through Freeze-Drying Method for Tissue Engineering Application



Shima Ghanavati Nasab and Abbas Teimouri*

Department of chemistry, Payame Noor University, Iran

Submission: June 29, 2017; **Published:** July 14, 2017

***Corresponding author:** Abbas Teimouri, Department of Chemistry, Payame Noor University, P.O. Box 81395-671, Iran, Tel: +98 31 33521804; Fax: +98 31 33521802; Email: a_teimouri@pnu.ac.ir, a_teimoori@yahoo.com

Abstract

In the present study, a novel scaffold containing chitosan (CTS), Montmorillonite (MMT) and Nano Zirconia (Nano ZrO₂) was prepared by the freeze drying method. The CTS/MMT/Nano ZrO₂ composite was characterized by SEM, XRD, TGA, BET and FT-IR studies. Cyto compatibility of the CTS/MMT/Nano ZrO₂ scaffold was assessed by MTT assay, revealing non-toxicity to the HGF cells. Thus, we suggest CTS/MMT/Nano ZrO₂ composite scaffold as a potential candidate for tissue engineering.

Keywords: Chitosan; Biomaterials; Nano composites; Composite materials; Tissue engineering; Montmorillonite; Nano ZrO₂

Abbreviations: MMT: Montmorillonite; XRD: X-ray Diffractometer; TG: Thermo Gravimetric; SEM: Scanning Electron Microscope.

Introduction

In recent years, many attempts have been made to place petrochemical products by biodegradable components. The most challenging part of this approach is to obtain bio-based materials with features equal to those of entirely synthetic products [1]. Biopolymers have privileges such as biodegradability and structural groups similar to natural extra cellular components [2]. Chitosan is a biopolymer derived from deacetylation of chitin and considered as an appropriate functional material for biomedical applications because of such great qualities as biocompatibility, non-antigenicity, biodegradability, antibacterial, blood coagulation and high mechanical strength, thereby making it suitable for tissue engineering [3-8]. To improve mechanical strength, chemical properties, dimensional stability and toughness of chitosan, it can be combined with clays such as Na-montmorillonite [9]. Or bio-inert ceramics like Zirconia [10].

Montmorillonite (MMT) is a kind of natural 2:1 type layered clay mineral. With only a low amount of MMT, the mechanical properties and solvent resistance of the composites can be strongly modified [11,12]. Also, polymer/layered silicate nano composites mostly exhibit considerably modified mechanical properties and solvent resistance of the composites can be

improved largely [11-14]. Zirconia (ZrO₂), a highly biocompatible ceramic and a chemically inert inorganic metal oxide with high stability, can increase the properties of chitosan upon the formation of the ZrO₂/chitosan composite [15-17]. At tissue level, zirconia has been discovered to be as biocompatible as titanium. Cultured osteoblasts are proliferated and differentiated on zirconia without producing any detrimental reaction [18].

In vivo studies have shown that ZrO₂ implants perform great osteointegration and zirconium-related materials, such as zirconia ceramics and coatings, have been used as bone implant materials [19]. In continuation of our recent study on the construction of composite scaffolds [20-22], we concentrated on the preparation and characterization of nano composite scaffolds CTS/MMT/Nano ZrO₂ to provide potential prospects of this nano composite for biomedical applications.

Materials and Methods

Chitosan (medium molecular weight) and Glutaraldehyde were purchased from Sigma-Aldrich. Montmorillonite was obtained from Shandong Longfeng Montmorillonite Co., China. Zirconium oxide nano powder was purchased from China Changsha Zhonglong Chemical (Group) Co., Ltd.

Preparation of CTS/MMT/ZrO₂ Nanocomposite Scaffold: The Chitosan (CTS), Montmorillonite and Nano Zirconia (ZrO₂) composite scaffold was prepared by the freeze drying method. To summarize, chitosan 2% (w/v) was dissolved in 1% acetic acid solution and then added to MMT/ZrO₂ (the amount of MMT was twice that of Nano ZrO₂) mixture suspension for 5 h to obtain the nano composites. After 1 h, 25% (v/v) Glutaraldehyde (for cross linking) was added to the mixture in a 1:32 volume ratio and stirred for another 1 h. Finally, the prepared solution was poured into a pre-cooled 24-well plate, frozen overnight at -80°C and then freeze dried in a lyophilizer for 24 h.

Evaluation of CTS/MMT/ZrO₂ nano composite scaffold properties: The structural morphology of the samples was evaluated using scanning electron microscope (SEM). The samples were analyzed using Philips X'PERT MPD X-ray diffractometer (XRD) with Cu α (1.5405 Å). A JASCO FT/IR-680 PLUS spectrometer was used to record IR spectra using KBr pellets. The BET specific surface areas and BJH pore size distribution of the samples were determined by adsorption-desorption of nitrogen at liquid nitrogen temperature by using a Series BEL SORP 18. To evaluate the weight loss of the CTS/MMT/ZrO₂ composite scaffold during thermo gravimetric (TG) analysis, a test was performed using a DuPont TGA 951 at temperatures ranging from room temperature to 1000 °C in air and at a heating rate of 10 °C/min.

Bioactive and cell adhesion study *in vitro*: The composite scaffolds were soaked in SBF according to the procedure described in Kokubo et al. [23]. Fibroblast cells were cultivated in culture flasks for 2 weeks, and cell suspension 2×10⁵ cells/cm² was seeded in scaffolds and cultured in 24-well plates. Cell-scaffolds were cultured in a humidified incubator. After 72 h, the cell-scaffolds were taken out and observed by SEM.

Results and Discussion

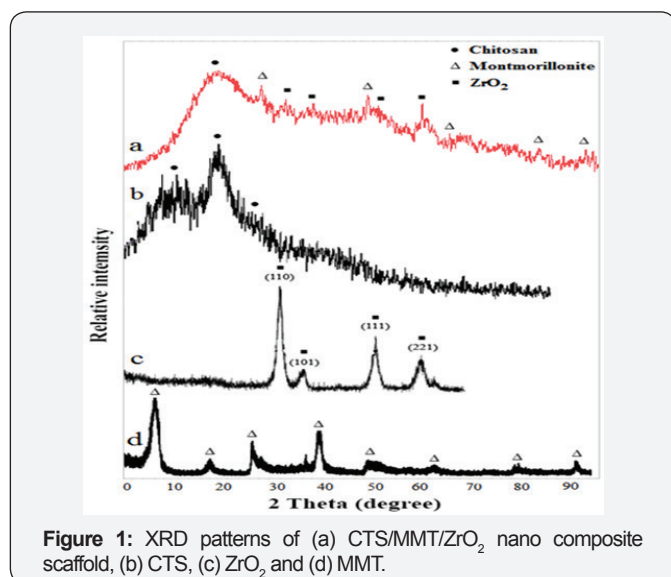


Figure 1: XRD patterns of (a) CTS/MMT/ZrO₂ nano composite scaffold, (b) CTS, (c) ZrO₂ and (d) MMT.

X-ray diffraction studies: As can be seen in (Figure 1) pure MMT typically showed a diffraction peak at 6.94°, while for CTS, the maximum was observed at 19°. In the XRD of ZrO₂, the sharp lines at 30.4, 51.0 and 60.2° were related to its tetragonal phase. Also, the XRD studies of CTS/MMT/ZrO₂ nano composite scaffold Figure 1a showed the characteristic peaks of chitosan (2 θ =19° and 22.5°), MMT (2 θ =28°) and ZrO₂ (2 θ =51° and 60.2°), there by suggesting the presence of them in the scaffold.

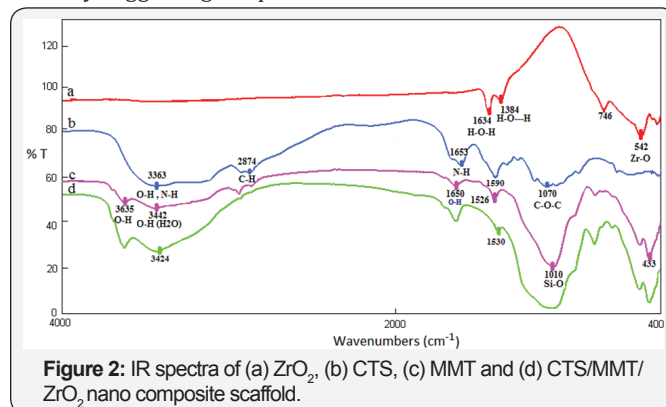


Figure 2: IR spectra of (a) ZrO₂, (b) CTS, (c) MMT and (d) CTS/MMT/ZrO₂ nano composite scaffold.

FT-IR analysis: Figure 2 shows the FTIR spectra of pure CTS, pure MMT, pure ZrO₂ and the prepared CTS/MMT/ZrO₂ nano composite scaffolds. The IR spectra of pure MMT had the band at 3635 cm⁻¹, which was related to the structural hydroxyl group vibration. Moreover, the bands at 1650 and 3442 cm⁻¹ were assigned to the bending and stretching vibrational modes of the hydrated O-H, respectively. Another band seen in MMT at 1010 cm⁻¹ was related to the Si-O bond. The IR spectra of the pure CTS represented the typical band at 3363 cm⁻¹, which was related to the stretching vibrations of the N-H and OH bonds. Also, the band at 1653 cm⁻¹ was related to the C=O bond of the acetyl group, while the band at 1070 cm⁻¹ corresponded to C-O-C bond [24]. The FTIR spectra of ZrO₂ indicated a significant band at 542 cm⁻¹ was assigned to the vibration of the Zr-O bond. From Figure 2d, it could be understood that the bands in CTS (O-H and N-H stretching), which could be seen to overlap with the bands of MMT (-OH was stretching of H₂O) at 3424 cm⁻¹, in addition to the band around 542 cm⁻¹, which was related to ZrO₂, could be observed in the IR spectra of the nano composite.

SEM analysis: The external morphology of CTS/MMT/ZrO₂ scaffold was investigated by SEM. The results gave a view on the porous structure of the scaffold and the distribution of pores. In this study, SEM was used to indicate any morphological changes in CTS/MMT/ZrO₂ scaffold surface after synthesis. (Figure 3) indicates the SEM images of CTS

- MMT
- ZrO₂
- CTS/MMT/ZrO₂ scaffold
- Chitosan.

Due to its extensive surface, could act as a bed/support for MMT and ZrO₂. It could be seen from (Figure 3d) that MMT

and ZrO_2 were scattered on the surface of CTS. The SEM image showed that the formation of scaffold was favoured, confirming

both the FT-IR and XRD analysis results.

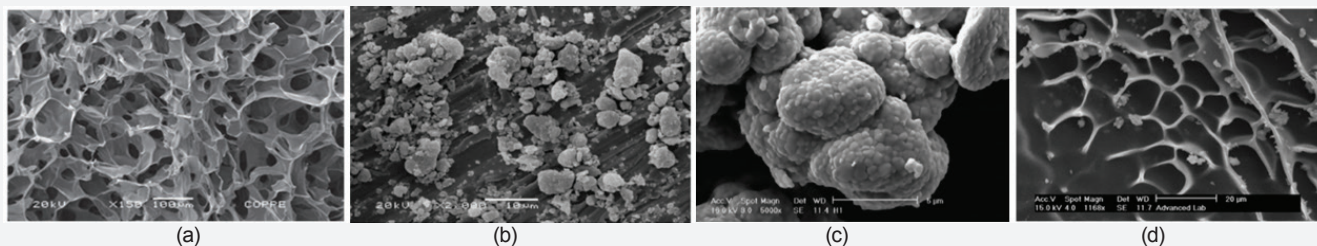


Figure 3: SEM images of (a) CTS, (b) MMT, (c) ZrO_2 and (d) CTS/MMT/ ZrO_2 nano composite scaffold.

BET Analysis: The nitrogen adsorption/desorption isotherm and the pore size distribution (inset) is shown in (Figure 4). The surface area was calculated by applying the BET equation to the isotherm [25] and the pore size distribution was estimated by BJH method [26]. The BET surface area, pore volume and average pore diameter were $12.180 \text{ m}^2\text{g}^{-1}$, $0.014 \text{ cm}^3 \text{ g}^{-1}$ and 0.994 nm , respectively. The sample was also mesoporous with N_2 adsorption-desorption isotherms of type IV and a H3 hysteresis loop according to IUPAC classification. The Type H3 loop, which does not display any limiting adsorption at high p/p° , is typically seen with the aggregates of plate-like particles giving rise to slit-shaped pores [27].

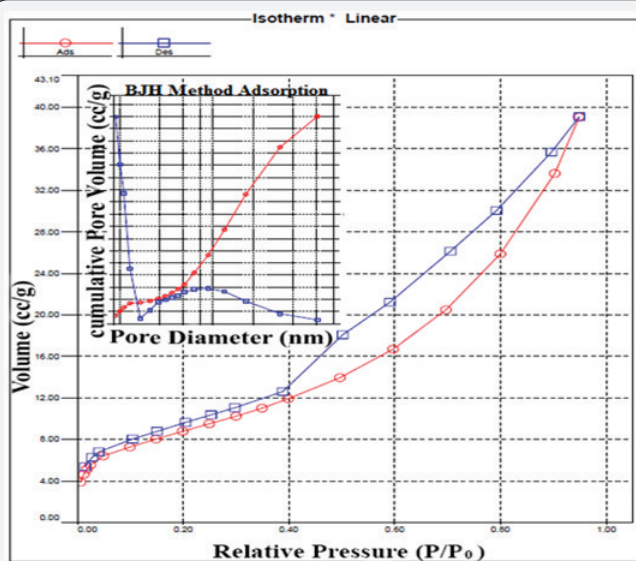


Figure 4: N_2 adsorption-desorption isotherm of CTS/MMT/Nano ZrO_2 . Inset: Pore size distribution using BJH method.

Thermal degradation: Thermal degradation of the scaffold was carried out using TGA (Figure 5). It can be seen from (Figure 5a) and (Figure 5b), the pure MMT and CTS/MMT began to decompose at around 450°C and 200°C , respectively. They were decomposed completely by the time the temperature reached 650°C . The thermal degradation of CTS/MMT/Nano ZrO_2 scaffold began to decompose at about 270°C and decomposed fully at 900°C . The results demonstrated that thermal stability for the CTS/MMT/Nano ZrO_2 was better than CTS, MMT and CTS/MMT.

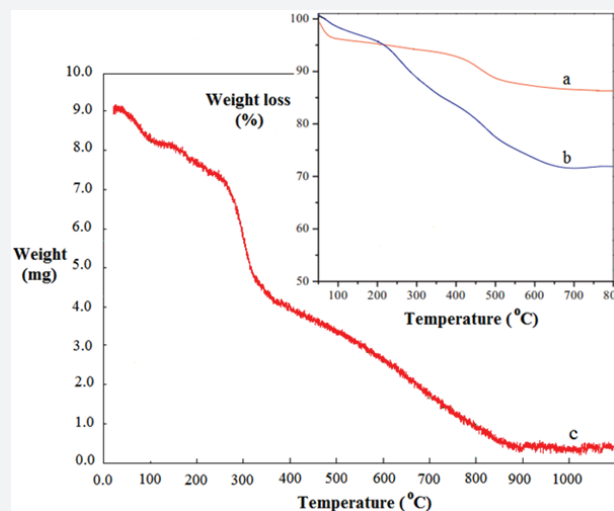


Figure 5: TG profiles of (a) MMT, (b) CTS/MMT and (c) CTS/MMT/Nano ZrO_2 .

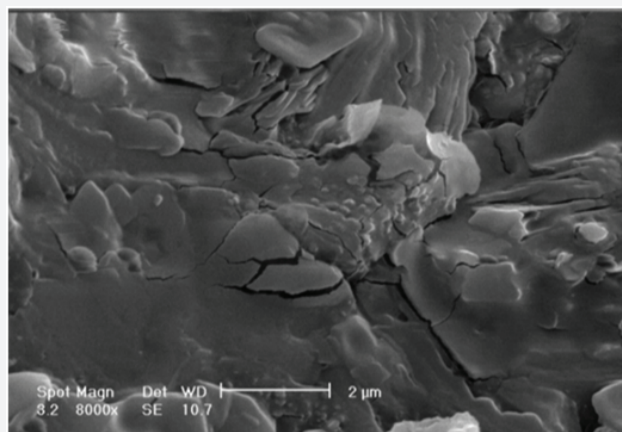
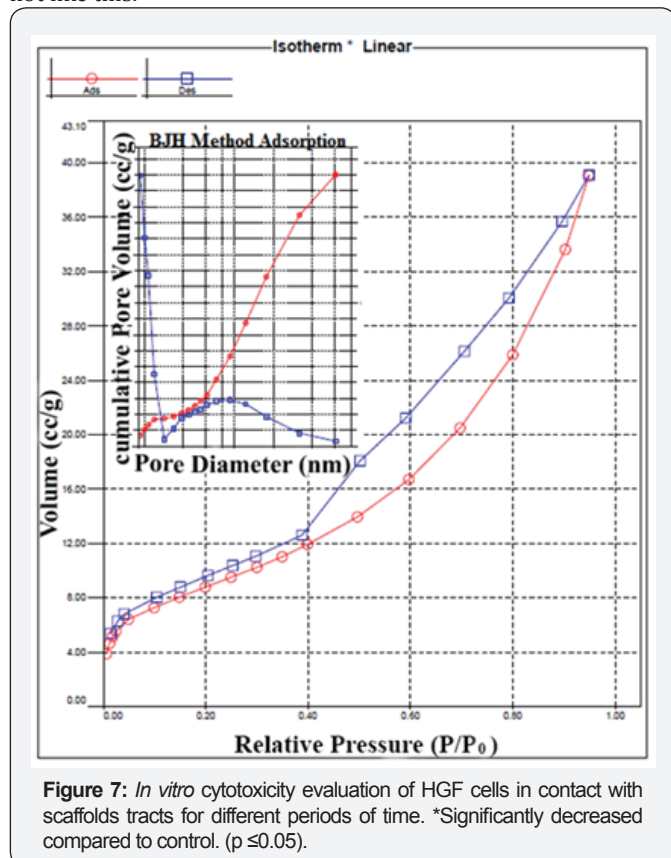


Figure 6: SEM image of apatite formation on CTS/MMT/ ZrO_2 14 days.

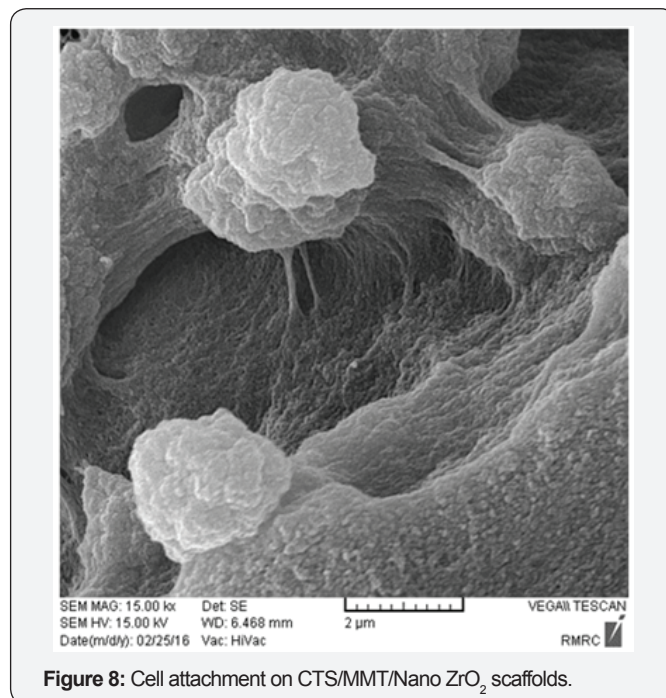
The *In vitro* bio-mineralization studies noted that the inclusion of zirconia enhanced the bio mineralization and bioactivity of the CTS/MMT/ ZrO_2 scaffold (Figure 6). Fibroblasts were cultured on the scaffold for 3 days. The results showed an increase in the cell activity in culture media containing CTS/MMT/ ZrO_2 scaffold during incubation, thereby indicating no cytotoxic effect on cell culture media.

In vitro evaluation of cytotoxicity: Cyto compatibility of the CTS/MMT/Nano ZrO₂ composite scaffolds was assessed using the MTT assay. The results propose that there are no significant toxic leachates in the CTS/MMT/Nano ZrO₂ scaffolds after incubation of the cells with the extract containing the leachates obtained after 24 and 72 h of incubation in the medium (Figure 7). No significant increase in cell growth was seen in the control, CTS, CTS/MMT and CTS/ Nano ZrO₂ groups after culturing for 72 h due to the space deficiency in the multi-well culture dishes, but the cells related to the composite groups were not like this.



From the results it can be concluded that a homogeneous incorporation of MMT and Nano ZrO₂ into CTS scaffold led to higher cell viability compared to that of the CTS-only scaffold or the CTS/MMT and CTS/ Nano ZrO₂ scaffold blended. Generally, the scaffolds prepared in this work were seen to possess favorable cell-compatible characteristics and can be considered as suitable materials for tissue engineering applications.

Cell attachment studies: SEM imaging was used to study the attachment and morphology of the cells on the scaffolds. (Figure 8) shows the SEM images of the cells after incubation for 24 h on the scaffolds and as shown in the Figure the cells attached and spread within the pore walls offered by the scaffolds. Cell attachment studies showed that the CTS/MMT/Nano ZrO₂ composite scaffold significantly increased the cell attachment which could largely attribute to the increase in its surface area, further supporting the suitability of these composite scaffolds for use in tissue engineering.



Conclusion

In this research, the novel CTS/MMT/ZrO₂ nano composite scaffold was fabricated by the freeze-drying method. The physicochemical properties of the composites were characterized by SEM, XRD, TGA, BET and FT-IR. The CTS/MMT/ZrO₂ scaffolds also showed biocompatibility with the fibroblast cells. The results indicated the prepared CTS/MMT/ZrO₂ scaffold could be a potential candidate for using in tissue engineering.

Acknowledgement

Supports from the Payame Noor University in Isfahan Research Council (Grant # 62370) are gratefully acknowledged.

References

1. F Croisier, Ch Jérôme (2013) Chitosan-based biomaterials for tissue engineering. *European Polymer Journal* 49(4): 780-792.
2. RAA Muzzarelli, V Baldassarre, F Conti, P Ferrara (1988) Biological activity of chitosan: ultrastructural study. *Biomater* 9(3): 247-9252.
3. RAA Muzzarelli, G Giacomelli (1987) The blood anticoagulant activity of N-carboxy methyl chitosan trisulfate. *Carbohydr Polym* 7(2) 787-796.
4. RAA Muzzarelli, Chitins (2009) Chitosans for the repair of wounded skin, nerve, cartilage and bone. *Carbohydr Polym* 76: 167-182.
5. R Jayakumar, N New, S Tokura, H Tamura (2007) Sulfated chitin and chitosan as novel biomaterials. *J Biol Macromol* 40(3): 175-181.
6. R Jayakumar, M Prabakaran, RL Reis, JF Mano (2005) Graft copolymerized chitosan-present status and applications. *Carbohydr Polym* 62: 142-158.
7. D Depan, AP Kumar, RP Singh (2009) Cell proliferation and controlled drug release studies of nanohybrids based on chitosan-g-lactic acid and montmorillonite. *Acta Biomater* 5(1): 93-100.
8. T Kean, M Thanou (2010) Biodegradation biodistribution and toxicity of chitosan. *Adv Drug Deliv Rev* 62(1): 3-11.

9. M Darder, M Colilla, E Ruiz-Hitzky (2003) Biopolymer-clay nanocomposites based on chitosan intercalated in montmorillonite. *Chem Mater* 15(20): 153774-3780.
10. S Pattnaik, S Nethala, A Tripathi, S Saravanan, A Moorthi, et al. (2011) Chitosan scaffolds containing silicon dioxide and zirconia nano particles for bone tissue engineering. *Int J Biol Macromol* 49(5): 1167-1172.
11. Y Kojima, A Usuki, M Kawasumi, A Okada, Y Fukushima, et al. (1993) Mechanical properties of Nylon 6-clay hybrid. *J Mater* 8(5): 1185-1189.
12. FH Lin, YH Lee, CH Jian (2002) A study of purified montmorillonite intercalated with 5-fluorouracil as drug carrier. *Biomater* 23: 1981-1987.
13. Y Kojima, YH Lee, A Usuki, M Kawasumi, O Kamigaito et al. (1993) Synthesis of nylon-6 clay hybrid. *J Mater* 8(5): 1179-1184.
14. M Kawasumi, N Hasegawa, A Okada (1997) Preparation and mechanical properties of polypropylene-clay hybrids. *Macromolecules* 30(20): 6333-6338.
15. L Kljajevic, B Matovic, A Radosavljevic-Mihajlovic (2011) Preparation of ZrO₂ and ZrO₂/SiC powders by carbo thermal reduction of ZrSiO₄. *J Alloys Compd* 509(5): 2203-2215.
16. HL Liu, XF Sun, CQ Yin, C Hu (2008) Removal of phosphate by mesoporous ZrO₂. *J Hazard Mater* 151(2-3): 616-622.
17. H Jiang, P Chen, Sh Luo, X Tu, et al. (2013) of novel nanocomposite Fe₃O₄/ZrO₂/chitosan and its application for removal of nitrate and phosphate. *Appl Surf Sci* 284: 942-949.
18. L Wang, RM Shelton, PR Cooper, M Lawson, JT Triffitt, et al. (2003) Evaluation of sodium alginate for bone marrow cell tissue engineering. *Biomaterials* 24(20): 3475-3481.
19. NVR Majeti (2000) A review of chitin and chitosan applications. *React Funct Polym* 46: 1-27.
20. A Teimouri, L Ghorbanian, A Najafi, R Emadi (2014) Fabrication and characterization of silk/forsterite composites for tissue engineering applications. *Ceram Int* 40: 6405-6411.
21. A Teimouri, R Ebrahimi, R Emadi, B Hashemi Ben, A Najafi (2015) Nano-composite of silk fibroin-chitosan/Nano ZrO₂ for tissue engineering applications: Fabrication and morphology. *Int J Biol Macromol* 76: 292-302.
22. A Teimouri, R Ebrahimi, A Najafi, R Emadi (2015) Fabrication and characterization of silk fibroin/chitosan/Nano γ -alumina composite scaffolds for tissue engineering applications. *RSC Adv* 5: 27558-27570.
23. T Kokubo, H Takadama (2015) How useful is SBF in predicting in vivo bone bioactivity?. *Biomater* 27: 2907-2915.
24. HL Liu, XF Sun, CQ Yin, C Hu (2008) Removal of phosphate by mesoporous ZrO₂. *J Hazard Mater*: 151(2-3): 616-622.
25. S Brunauer, PH Emmett, E Teller (1938) Adsorption of Gases in Multi molecular Layers. *J Am Chem Soc* 60: 309-319.
26. SJ Gregg, KSW Sing (1982) Adsorption, Surface Area and Porosity. In: editors (Eds.) Academic Press (2th edn) New York, USA.
27. KSW Sing, DH Everett, RA W Haul, L Moscou, RA Pierott (1985) Reporting physisorption data for gas/solid systems with special reference to the determination of surface area and porosity. *Pure Appl Chem* 57(4): 603-619.



This work is licensed under Creative Commons Attribution 4.0 License
DOI: [10.19080/OMCIJ.2017.03.555601](https://doi.org/10.19080/OMCIJ.2017.03.555601)

Your next submission with Juniper Publishers will reach you the below assets

- Quality Editorial service
- Swift Peer Review
- Reprints availability
- E-prints Service
- Manuscript Podcast for convenient understanding
- Global attainment for your research
- Manuscript accessibility in different formats (Pdf, E-pub, Full Text, Audio)
- Unceasing customer service

Track the below URL for one-step submission
<https://juniperpublishers.com/online-submission.php>